

## Correlation of ADC With Pathological Treatment Response for Radiation Therapy of Pancreatic Cancer



Entesar Dalah<sup>\*,†</sup>, Beth Erickson<sup>\*</sup>, Kiyoko Oshima<sup>‡</sup>, Diane Schott<sup>\*</sup>, William A. Hall<sup>\*</sup>, Eric Paulson<sup>\*,§</sup>, An Tai<sup>\*</sup>, Paul Knechtges<sup>§</sup> and X. Allen Li<sup>\*</sup>

<sup>\*</sup>Department of Radiation Oncology, Medical College of Wisconsin, Milwaukee, WI, USA; <sup>†</sup>Department of Medical Diagnostic Imaging, College of Health Science, University of Sharjah, UAE; <sup>‡</sup>Department of Pathology, Medical College of Wisconsin, Milwaukee, WI, USA; <sup>§</sup>Department of Radiology, Medical College of Wisconsin, Milwaukee, WI, USA

### Abstract

**PURPOSE:** To investigate the feasibility of using apparent diffusion coefficient (ADC) to assess pathological treatment response in pancreatic ductal adenocarcinoma (PDAC) following neoadjuvant chemoradiation (nCR). **MATERIALS/METHODS:** MRI and pathological data collected for 25 patients with resectable and borderline resectable PDAC following nCR were retrospectively analyzed. Pre- and post-nCR mean ADC values in the tumors were compared using Wilcoxon matched pairs test. Correlation of pathological treatment response and ADC values was assessed using Pearson's correlation coefficient test and receiver-operating-curve (ROC) analysis. **RESULTS:** The average mean and standard deviation (SD) of the ADC values for all the patients analyzed were significantly higher in post-nCR ( $1.667 \pm 0.161 \times 10^{-3}$ ) compared with those prior to nCR ( $1.395 \pm 0.136 \times 10^{-3}$  mm<sup>2</sup>/sec), ( $P < 0.05$ ). The mean ADC values after nCR were significantly correlated with the pathological responses ( $r = -0.5172$ );  $P = 0.02$ . The area under the curve (AUC) of the ADC values for differentiating G1, G2 and G3 pathological responses, using ROC analysis, was found to be 0.6310 and  $P = 0.03$ . **CONCLUSION:** Changes of pre- and post-treatment ADC values significantly correlated with pathological treatment response for PDAC patients treated with chemoradiation therapy, indicating that the ADC could be used to assess treatment response for PDAC.

*Translational Oncology (2018) 11, 391–398*

### Introduction

Pancreatic ductal adenocarcinomas (PDACs) are known to progress rapidly, are often diagnosed at an advanced stage [1] and are generally challenging for early treatment response assessment [2]. Histopathologically, PDAC is distinguished by a prominent desmoplastic reaction, a process in which fibrous tissue infiltrates and envelops neoplasms, adding to the difficulty of early diagnosis [3]. When such cancer tissue is treated with radiation therapy (RT), local tissue damage will be induced. However, normal tissue that is mixed within the vicinity of tumor tissue tends to overcome some of the damage through a process called regeneration. If tumor vasculature fails to regenerate normally, i.e., create normally structured and functioned-cells, then, the tissue is repaired and replaced by scarred fibrosis/fibroblasts tissue [4,5] that can be seen by appropriate histological stains.

The apparent diffusion-coefficient (ADC) map obtained from diffusion-weighted (DW) magnetic resonance imaging (MRI) reflects overall diffusivity of water molecules within tissue at the cellular level.

ADC depends on a number of factors, including water mobility in the intra- and extracellular space, the relative volume of the extravascular extracellular space, cellular membrane integrity, macromolecular components and permeability [6]. ADC values have been correlated with cellularity in brain cancer [7] and hepatocellular carcinoma [8] where low-ADC values were observed in dense and fibrotic tumors due to increased tissue cellularity and reduced extravascular

Address all correspondence to: X. Allen Li, PhD, Department of Radiation Oncology, Medical College of Wisconsin, 8701 Watertown Plank Road, Milwaukee, WI 53226. E-mail: [ali@mcw.edu](mailto:ali@mcw.edu)

Conflicts of Interest Notification: Do not exist.

Received 1 December 2017; Revised 11 January 2018; Accepted 16 January 2018

© 2018 The Authors. Published by Elsevier Inc. on behalf of Neoplasia Press, Inc. This is an open access article under the CC BY-NC-ND license (<http://creativecommons.org/licenses/by-nc-nd/4.0/>). 1936-5233/18

<https://doi.org/10.1016/j.tranon.2018.01.018>

extracellular space volume. Several studies have demonstrated the potential of using DW-MRI to detect and measure cellular changes that occur in response to chemoradiation therapy in diffuse malignant gliomas [9,10] and primary bone tumors [11]. Current imaging assessment of tumor response to neoadjuvant chemoradiation (nCR) relies primarily upon changes in tumor size; this requires significant time due to the relatively slow removal of tumor macromolecular debris after cell death [2]. Subsequently, it would be advantageous to detect individual cellular changes in the early phase of treatment course, allowing for highly individualized treatment adaptation.

Herein, we study the ability of ADC value to assess cellular changes in PDAC patients receiving nCR treatment. The cellular changes observed with ADC value will be validated with the pathological treatment response assessment of resectable and borderline resectable PDAC patients.

## Material and Methods

Imaging and pathologic data for a total of 25 patients with histologically confirmed resectable and borderline resectable PDAC in the pancreatic head were retrospectively reviewed.

### MRI Data

MRI simulation for RT planning was performed on a 70-cm bore, 3T scanner (Verio, Siemens, Erlangen, Germany) with the patient setup in treatment position on a flat tabletop insert. The integrated body radiofrequency (RF) coil was used for signal transmission and the combination of a spine phased-array RF coil and two flexible phased-array RF coils was used for signal reception. Respiratory triggering was applied at the 50% phase of the respiratory cycle, corresponding to end of expiration. A two-dimensional, single-shot, twice-refocused spin-echo, echo-planar imaging sequence was used for DWI acquisition, along with the following parameters: pixel size,  $1.4 \times 1.4 \text{ mm}^2$ ; matrix (MAT),  $256 \times 160$ ; time to echo (TE), 60 ms; time to repetition (TR), 10,000 ms; generalized autocalibrating partially parallel acquisition (GRAPPA) (R=2); number of excitations (NEX), four; slice thickness (TH), 8 mm;  $b = 0, 500, 1000 \text{ s/mm}^2$ .

### Pathological Treatment Response and Tumor Size

After pancreatic surgery/tumor resection, the surgical specimens were fixed in formalin overnight and subsequently, the gross examination was performed. The areas of tumor and surrounding fibrosis in the head of the pancreas were serially sectioned. Hematoxylin and eosin sections were prepared and treatment effect was evaluated microscopically. An example of such a pathological assessment of the surgical specimen is shown in Figure 1A. The College of American Pathologists (CA3P) grading system [12] was used to evaluate the extent of residual tumor as follows: Grade 0 (G0) for complete response (no viable cancer cells), Grade 1 (G1) for moderate response (single cells or small groups of residual cancer cells in extensive fibrosis), Grade 2 (G2) for minimal response (residual cancer outgrown by fibrosis) and Grade 3 (G3) for poor response (extensive residual cancer). The pathologist provided the measurement of the largest dimension of continuous tumor lesion. In a case of multiple foci of a discontinuous tumor, the largest focus was measured.

### Gross Tumor Volume Delineation

Custom software was used to generate ADC parameter maps from the native DWI, using a noise threshold of 2%, and a montage of the  $b = 0 \text{ s/mm}^2$  and  $b = 1000 \text{ s/mm}^2$ . DWI images and ADC parameter

maps were transferred offline and post-processed, using software (MIM, version 6.4.5; Cleveland, OH, USA). Pre- and post-nCR gross tumor volume (GTV) on the DWI and ADC were manually delineated from regions confined within the pancreas head with hyperintensity appearance characteristics on DWI and hypointensity on ADC maps.

### Treatment Response Assessment

ADC value change was assessed over two time points, pre- and post-nCR, for the 23 patients who had MRI scans and underwent surgery after completing the nCR therapy. The histogram of ADC values in all the voxels inside the ADC-defined GTV was used to calculate the mean ADC values, as well as their standard deviation (SD). In addition, the volumes of pre- and post-nCR GTVs were calculated and the post-nCR ADC tumor maximum dimensions (TMD) were measured, using an automated function in MIM (MIM Software Inc.) called RECIST and compared to the pathologically defined tumor size. RECIST provides a robust and reproducible measure of TMD, which is based on the GTV center of mass.

An automatic outlier eliminating nonlinear two-component Gaussian-fitting method was used to separate cancer-related tissue (i.e., cellularity) from fibrosis (i.e., scars) tissue inside the GTV and compared with pathological treatment assessments for all 25 patients. Although one can make more than a two-component Gaussian fit, patients' pathological treatment response grading was reported in terms of cellularity and fibrosis, thus, the choice of two-component was made to allow validation. The two-component Gaussian fit peaks were arranged as such: the lowest-ADC value was assigned for cellularity and the highest-ADC value for fibrosis. From peaks amplitude, i.e., peak 1 and 2, the fraction of cellularity to fibrosis component occupying the GTV was also calculated, which was mathematically defined as:

$$\text{Fraction of component 1} = \frac{\text{Peak 1 amplitude}}{\text{Peak 1 amplitude} + \text{Peak 2 amplitude}},$$

and fraction of component 2 = (1 - fraction of component 1).

### Statistical Analysis

Mean ADC value, pathological treatment response and histograms of post-nCR ADC values for the patients studied were transferred to Prism (version 6; GraphPad Software, La Jolla, CA) for statistical analysis. A Wilcoxon matched pairs test was used to determine whether significant differences existed between pre- and post-nCR mean ADC values and between TMD defined by ADC-GTV and pathological reported values. A Pearson's correlation coefficient test was used to determine the correlation of pathological treatment response (cellularity) and mean ADC values. Additionally, receiver-operating-characteristic curve (ROC) analysis was used to calculate the area under the curve (AUC) of the ADC values for differentiating G1, G2 and G3 cases. For all statistical tests,  $P=0.05$  was used for significance.

## Results

All 25 patients underwent surgery after completing the nCR therapy. Per our institutional protocol, these patients were treated with chemotherapy (gemcitabine or Xeloda, and FOLFIRINOX or gemcitabine-Abraxane) and RT (50.4 Gy delivered in 28 fractions, using intensity-modulated radiation therapy [IMRT]). All 25 patients had post-nCR MRI, while 23 had both pre- and post-nCR DW-MRI

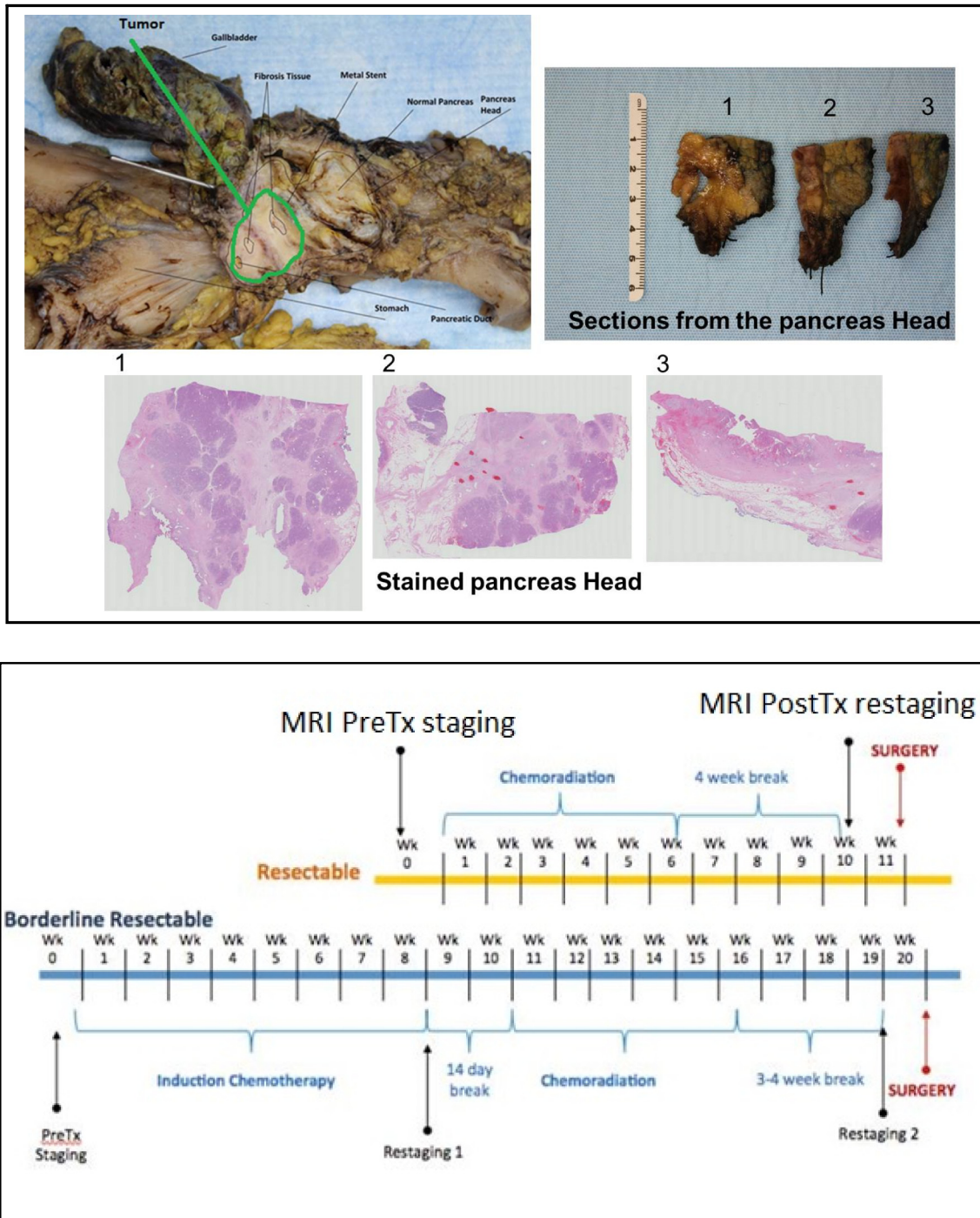


**Figure 1.** (A) An example of pathological assessment of surgical specimen (top); and (B) a scheme of the neoadjuvant chemoradiation(nCR) treatment management and MRI staging and restaging scan for resectable and borderline resectable pancreatic ductal adenocarcinoma patients (bottom).

data. All 25 patients underwent surgery on an average of 34 days, ranging from 29 to 50 days, after completing the nCR treatment. The average duration from post-nCR MRI scan to the surgery was eight days, ranging from five to 16 days. The average duration from nCR completion to post-nCR MRI scan was 27 days, ranging from 18 to 43 days. The average duration from completion of RT to the post-MRI scan was 25 days, ranging from 21 to 50 days. The treatment management schedules, including chemoradiation therapy, pre- and post-MRI scans and surgery for both resectable and

borderline resectable cases, are shown in Figure 1 and patient characteristics are presented in Table 1.

**ADC Value Changes**

The comparison of the mean ADC values in the GTVs, defined based on the ADC map, for the two timepoints, pre- and post-nCR, indicates that the average mean and SD of the ADC values for the 23 patients analyzed were significantly higher in post-nCR ( $1.667 \pm 0.161 \times 10^{-3}$ ) compared with those pre-nCR ( $1.395 \pm 0.136 \times 10^{-3}$ )

**Table 1.** Patient Characteristics, Pre-ADC Defined GTV and CT Based GTV for Comparisons

Total sample size	25
Tumor location	Pancreas head
Treatment effect grading	
G1	3 (12 %)
G2	16 (64%)
G3	6 (14%)
Tumor status	
Resectable	3
Borderline	22
No. of patients with pre and post ADC	23 (92%)
No. of patient with post ADC	25 (100%)
Pathology tumor maximum dimension (TMD)	2.5 (1.6 – 3.8) cm
Pre-ADC defined GTV, mean and range	19.4 (7.4 – 36.8) cm <sup>3</sup>
Pre-CT defined GTV, mean and range	40.8 (9.61 – 228.2) cm <sup>3</sup>

mm<sup>2</sup>/sec) GTVs ( $P < 0.05$ ). In addition to quantitative changes in pre- and post-nCR ADC values, spatial changes in the ADC map (heterogeneity) were also observed. Figure 2 presents comparisons of pre- and post-ADC maps for a sample case with the moderate response (G2), where stent was included in the manually defined pre-GTV (hypointense), and due to GTV shrinkage, the stent was excluded in the post-GTV (hyperintense). While stent artifact is generally challenging. It has been shown that considerable artifact was seen in DWI with stainless steel stent, but not in the nitinol containing stents [2]. Thus, effort was made to avoid using stainless steel stent.

### Morphological Changes

GTV shrinkage was dominant in all 23 patients with MRI data, Figure 3. The average mean and SD of the GTV volumes analyzed were significantly smaller in post-nCR ( $9.75 \pm 5.93$  cc) compared with those in pre-nCR ( $37.79 \pm 12.1$  cc) GTVs ( $P < 0.05$ ), based on the Wilcoxon test. In contrast, tumor volume change of up to 40% during chemoradiation as measured from daily CT was reported by Chen et al, [13]. Post-nCRADC-defined TMD was generally larger than the pathologically defined tumor size, with a mean difference of ~ 6 mm ranging from four to 17 mm. Detailed discussion on GTV delineation variability using multimodality imaging including 3D/4D CT, dynamic contrast enhanced (DCE)-MRI, ADC-MRI, and PET/CT for RT of pancreatic cancer was addressed in a previous work by Dalah et al [14]. The mean difference (range) in the measurements of maximum diameter of GTV from DCE-MRI, and ADC-MRI compared with pathologic specimens for a total of 8 patients were 0.84 (2.24 to 0.9), 0.41 (0.15 to 2.3) cm, respectively. The mean differences and difference ranges between the GTV of DCE-MRI, and ADC-MRI, and the GTV from 3D/4D CT were found statistically different with  $-37.26$  ( $-76.20$  to  $-5.32$ ),  $-31.24$  ( $-79.40$  to  $-6.40$ ) cm<sup>3</sup>, respectively, indicating 3D/4D CT defined GTV were larger than DCE-MRI and ADC-MRI. This finding is realistic given the CT defined GTV is based on delineating the whole pancreas head rather than the gross tumor nested inside the pancreas head.

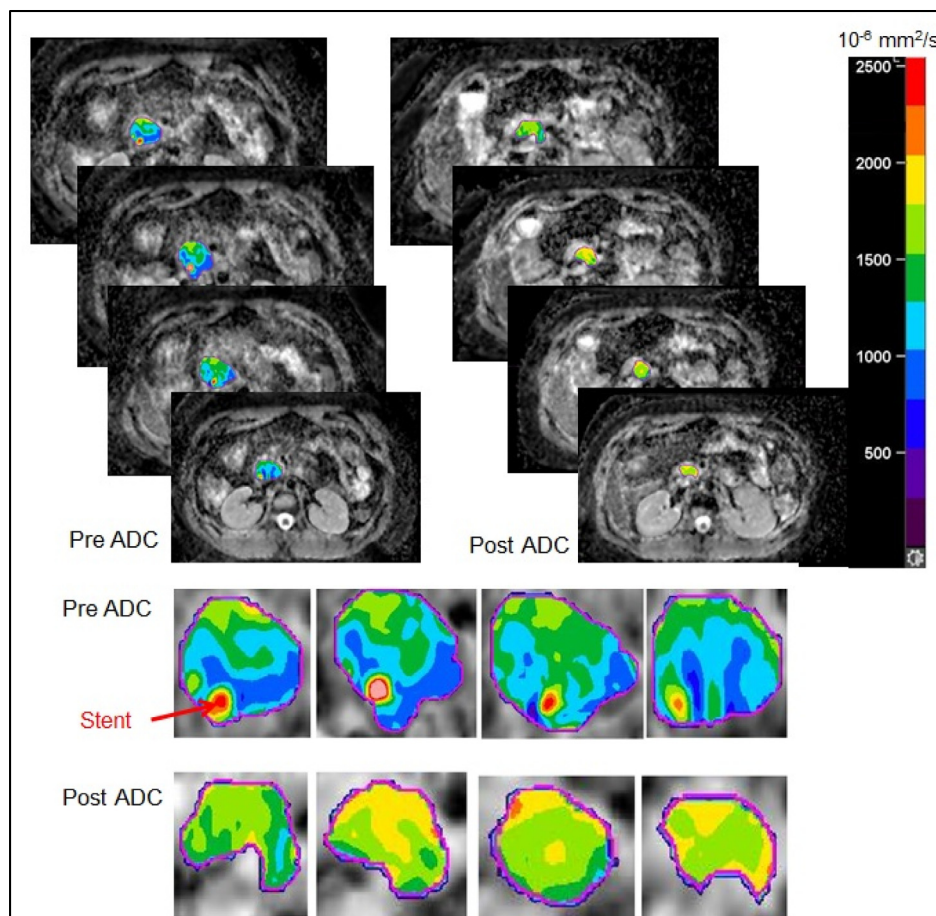


**Figure 2.** Slice-to-slice comparison of the pre- and post-nCR ADC maps. Change in spatial heterogeneity of ADC values before and after the nCR for a pancreatic head tumor with pathologically proven moderate response (G2) is shown.

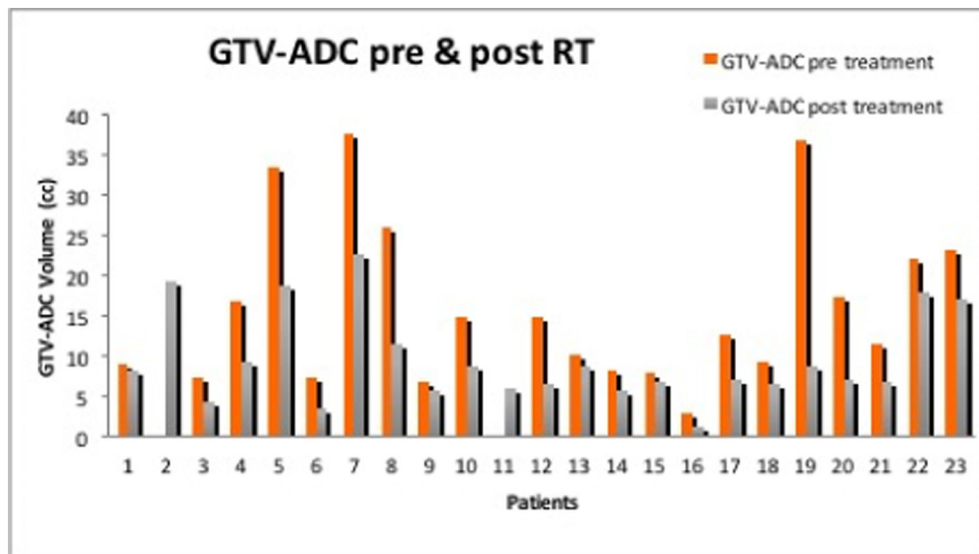


**Figure 3.** Gross tumor volume (GTV) delineation based on ADC map demonstrating general tumor shrinkage post-nCR.

### *Pathologically validated*

The mean post-nCR ADC values for all 25 patients correlated significantly with the pathologic treatment response cellular changes, with  $r=-0.5172$  and  $P<0.05$ . The area under the curve (AUC) of the ADC values for differentiating G1, G2 and G3 cases using ROC analysis was found to be 0.6310 and  $P=0.03$ . Figure 4A presents the correlations of pathological response (cellularity) with the mean post-nCR ADC values and the stained pictures of all three categories with G1 showing single cells or small clusters of residual cancer cells in extensive fibrosis, G2 demonstrating residual cancer outgrown by fibrosis and G3 evidencing extensive residual cancer. These were read under Hematoxylin & Eosin Stain, 200 magnification powers. The color wash post-nCR ADC map clearly demonstrates cellular heterogeneity across the GTV, with higher ADC values dominating in G1 pathologically defined surgery specimens and moderate- and low-ADC values predominating in G2, and G3, respectively. This finding also has been confirmed with the GTV voxel histograms of samples of G1, G2 and G3 responding patients, as shown in Figure 4B).

### *Cellularity Versus Fibrosis*

Histograms of post-nCR ADC-defined GTV for all 25 patients were fitted by automated outlier eliminating nonlinear Gaussian regression based on pathological treatment effect that is graded according to tumor cells destruction i.e., cellularity and fibrosis regions (Figure 5). The amplitude, mean and SD for each compartment (peak 1 and peak 2) were computed. The average mean and SD of the ADC values, as well as the average fraction of occupied component in these ADC-defined cellularity and fibrosis regions were  $1.801 \pm 0.116 \times 10^{-3}$  (37%) and  $2.039 \pm 0.250 \times 10^{-3}$  (63%) for the G1 cases,  $1.566 \pm 0.144 \times 10^{-3}$  (44%) and  $1.657 \pm 0.112 \times 10^{-3}$  (56%) for G2 and  $0.470 \pm 0.0635 \times 10^{-3}$  (79%) and  $0.903 \pm 0.962 \times 10^{-3}$  (21%) for G3, respectively. Figure 5 presents the mean post-nCR ADC values for the cellularity and fibrosis regions for the G1, G2 and G3 responses. Treatment response heterogeneity among individuals is expected, which is thought to be related to the

heterogeneous nature of tumor aggressiveness, individuals physiological and biological status. We believe that the patient heterogeneity causes the change of the mean ADC values for both fibrotic portion and cellular portion with respect to different response grades. A sample ADC histogram, along with the two Gaussian-fitting peaks, is included in Figure 5.

### **Discussion**

A desmoplastic reaction is a distinctive histopathologic finding in PDAC. The abundant growth of fibrotic tissue through secretion of collagen (protein) infiltrates and encases neoplasms causing a remarkable dense extracellular matrix component [3], which limits the delivery of radiosensitizing systemic therapy and reduces the amount of oxygen available for radiation-induced free radical formation, thereby decreasing the effectiveness of chemoradiation [15]. The presence of an adequate oxygen tension, of approximately 25–30 mmHg, significantly increases the lifetime of these toxic free radicals, leading to a more effective radiotherapy outcome [16]. This explains the profound resistance of this cancer to treatment and the challenge of early treatment response assessment. In radiation therapy, as more cells become damaged by radiation, more scarring and fibrosis are created due to failing regeneration. This causes viable tissue to be replaced by fibrotic tissue, which is considered an indication of a successful treatment.

ADC, calculated from diffusion-weighted MRI, provides useful information about tumor cellularity, permeability and membrane integrity [6]. In neoplasms, a decrease in ADC has been shown to correlate with an increase in cellularity in certain tumor types [7,8,17]. In contrast, an increase in ADC has been considered an indication of successful treatment in gliomas and primary bone tumors [9–11]. Changes in diffusion parameters measured one week after initial treatment were significantly correlated with later response or no response in patients with brain tumors [9]. The rationale behind delineating the GTV on the ADC map instead of the DWI is to eliminate the T2 shine-through effect, which refers to a high signal on DWI that is not related to restricted diffusion, but rather to high T2 signal associated with long T2 decay time in some normal tissues.

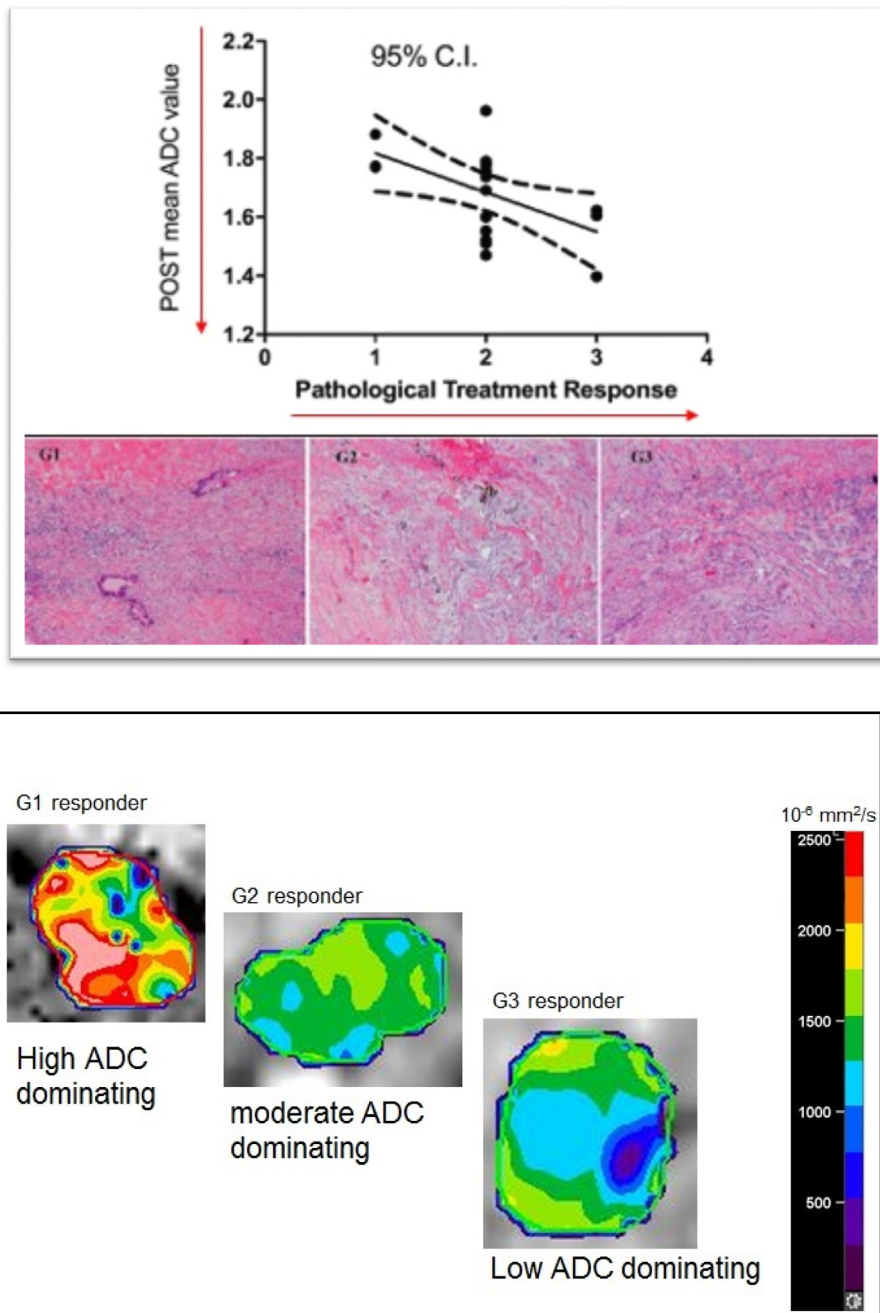


**Figure 4.** (A) Significant correlations (top) of pathological treatment response with the mean post-nCR ADC values and the stained pictures (bottom) of all three categories shown with G1 single cells or small clusters of residual cancer cells in extensive fibrosis, G2 residual cancer outgrown by fibrosis, and G3 extensive residual cancer. (B) Spatial post-nCR ADC value heterogeneity in relation to treatment response (cellularity as a result of failing regeneration) together with histogram data for all three-tumor response grading.

In this pilot study, we found significant correlation between the change of ADC values before and after treatment and pathological treatment response in patients with PDAC following neoadjuvant chemoradiation. The analysis of pre- and post-nCR ADC histograms demonstrated a shift toward higher-ADC values in tumor that pathologically showed good response to nCR treatment. The nonlinear Gaussian regression analysis may allow distinguishing different tissue characteristics based on their water-restricted diffusion in the GTVs. The two ADC values obtained from the two compartments may be assigned for water-restricted diffusion from

1) the cancer tissue (cellularity) left in the tumor vicinity and 2) the fibrotic tissue that resulted from failure to regenerate normal tissue. Figure 4A demonstrates a negative significant relationship between mean ADC values in association with pathological treatment response findings while Figure 5 demonstrates a reasonably clear trend between cellularity versus fibrosis obtained from fitting and that of the pathological response grading system. In addition, the average occupied fraction of cellularity to fibrosis that was calculated from the peaks amplitude demonstrates higher percentage of fibrosis (63%) to cellularity (37%) in G1-responding patients, while there is a higher

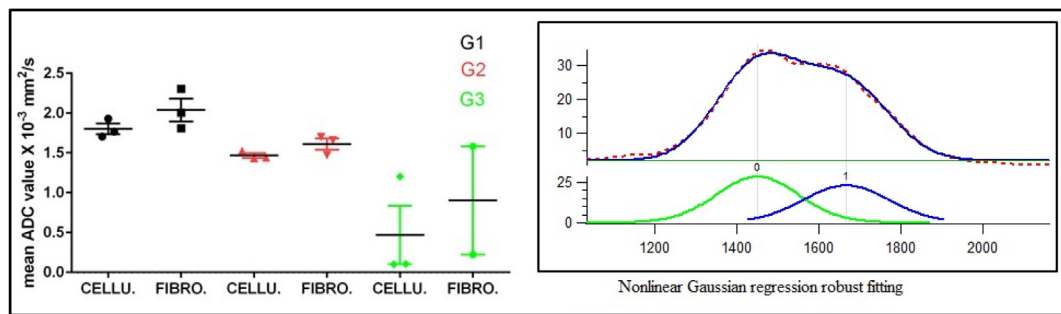


**Figure 5.** The mean post-nCR ADC values (left) for the cellularity and fibrosis regions, as divided by nonlinear Gaussian regression fitting, for the G1, G2 and G3 responses. A sample ADC histogram with two Gaussian fitting curves is included (right).

percentage of cellularity (79%) to fibrosis (21%) in G3-responding patients. Based on this finding, it is reasonable to assume that the lower-ADC values obtained from the nonlinear Gaussian regression are associated with more cancer residuals (cellularity), whereas the higher ADC values from the same fitting are raised from the water restriction of the fibrotic tissue in the GTV, which also agrees with Muraoka et al [17]. This group [17] found a correlation between preoperative ADC values in cancerous and noncancerous tissue, with low-ADC values indicating cancerous tissue and high-ADC values indicating noncancerous tissue. However, the large amount of fibrotic tissue in the Muraoka et al [17] study refers to the desmoplastic reaction of pancreatic tumors rather than failed regeneration, as the study was conducted in preoperative patients. In this pilot study that involves postoperative patients, the ADC values representing the fibrosis (scars) are shown to be more dominant than the ADC values representing the cellularity, at least, for the good- and moderate-responding patients. These preliminary findings suggest that the ADC map may be used as a potential surrogate for treatment response in pancreatic adenocarcinoma patients.

An early treatment response assessment for patients with pancreatic cancer is highly desirable, offering the potential to adapt therapy to the patient-specific response. The ability to identify spatially varying ADC changes within the GTV during RT delivery would allow treatment modification so that a higher radiation dose may be delivered to the non- or poor-responding regions within the GTVs.

To our knowledge, a limited number of reports have looked at ADC parameter maps in pancreatic adenocarcinoma. A few retrospective studies found that tumors with low-ADC values responded poorly to systemic therapy [2,18], consistent with our current findings. Kurosawa et al [19] identified preoperative ADC values as a significant prognostic factor after surgery for resectable patients. Nishiofuku et al [20] found that the longitudinal changes of ADC values throughout the course of chemotherapy, i.e., four weeks, were the strongest predictor of prognosis-free survival in unresectable patients. A major limitation in our study is the small patient number. A larger sample size is needed to establish a cutoff value and the thresholding method to distinguish cellularity from fibrosis for G1, G2 and G3 pathologically responding patients, given that a statistically significant correlation exists between ADC value and tumor cellularity, whether originating from desmoplastic reactions or failing regeneration. Our primary endpoint was the pathologic response, according to the grading system developed by Washington et al [12]. Larger studies will be required to establish a

standardized response criteria specific for ADC parameter maps, similar to that of RECIST and PRECIST1.0.

## Conclusions

Changes between pre- and post-treatment ADC radiomic parameters (e.g., mean ADC) were found to correlate with pathological treatment response for pancreatic adenocarcinoma patients treated with chemoradiation. These data reflect that ADC values acquired following a course of chemoradiation could be used to predict tumor pathologic response and improve the selection of patients who could preferentially benefit from therapeutic intensification.

## Acknowledgement

This work is partially supported by MCW Cancer Center Meinerz Foundation and by Elekta Inc.

## References

- [1] Bachem M, Schünemann M, Ramadani M, Siech M, Beger H, Buck A, Zhou S, Schmid-Kotsas A, and Adler G (2005). Pancreatic Carcinoma Cells Induce Fibrosis by Stimulating. *Gastroenterology* **128**, 907–921.
- [2] Cuneo KC, Chenevert TL, Ben-Josef E, Feng MU, Greenson JK, Hussain HK, Simeone DM, Schipper MJ, Anderson MA, and Zalupski MM, et al (2014). A Pilot Study of Diffusion-Weighted MRI in Patients Undergoing Neoadjuvant Chemoradiation for Pancreatic Cancer. *Transl Oncol* **7**, 644–649.
- [3] Mahadevan D and Von Hoff D (2007). Tumor-Stroma Interactions In Pancreatic Ductal Adenocarcinoma. *Mol Cancer Ther* **6**, 1186–1197.
- [4] Meran S, Thomas DW, Stephens P, Enoch S, Martin J, Steadman R, and Phillips AO (2008). Hyaluronan Facilitates Transforming Growth Factor-1-mediated Fibroblast Proliferation. *J Biol Chem* **283**, 6530–6545.
- [5] Lee JJ, Pererac RM, Wang H, Wu DC, Liu S, Han S, Fitamant J, Jones PD, Ghanta KS, and Kawano S, et al (2014). Stromal Response To Hedgehog Signaling Restrains Pancreatic Cancer Progression. *Proc Natl Acad Sci U S A*. <https://doi.org/10.1073/PNAS.1411679111>.
- [6] Thoeny HC and Ross BD (2010). Predicting and Monitoring Cancer Treatment Response with Diffusion-Weighted MRI. *J Magn Reson Imaging* **32**, 2–16.
- [7] Ellingson BM, Malkin MG, Rand SD, Connelly JM, Quinsey C, LaViolette PS, Bedekar DP, and Scaiminda KM (2010). Validation of Functional Diffusion Maps (fDMs) as a Biomarker for Human Glioma Cellularity. *J Magn Reson Imaging* **31**, 538–548.
- [8] Yu JI, Park HC, Lim DH, Choi Y, Jung SH, Paik SW, Kim SH, Jeong WK, and Kim YK (2014). The Role of Diffusion-Weighted Magnetic Resonance Imaging in the Treatment Response Evaluation of Hepatocellular Carcinoma Patients Treated With Radiation Therapy. *Int J Radiat Oncol Biol Phys* **89**, 814–821.
- [9] Mardor Y, Pfeffer R, Spiegelmann R, Roth Y, Maier SE, Nissim O, Berger R, Glicksman A, Baram J, and Orenstein A, et al (2003). Early Detection of Response to Radiation Therapy in Patients with Brain Malignancies Using Conventional and High b-Value Diffusion-Weighted Magnetic Resonance Imaging. *J Clin Oncol* **21**, 1094–1100.

- [10] Hamstra DA, Chenevert TL, Moffat BA, Johnson TD, Meyer CR, Mukherji SK, Quint DJ, Gebarski SS, Fan X, and Tsien CI, et al (2005). Evaluation Of The Functional Diffusion Map As An Early Biomarker Of Time-To-Progression And Overall Survival In High-Grade Glioma. *Proc Natl Acad Sci U S A*. <https://doi.org/10.1073/PNAS.0508347102>.
- [11] Hayashida Y, Yakushiji T, Awai K, Katahira K, Nakayama Y, Shimomura O, Kitajima M, Hirai T, Yamashita Y, and Mizuta H (2006). Monitoring Therapeutic Response Of Primary Bone Tumors By Diffusion-Weighted Image: Initial Results. *Eur Radiol* **16**, 2637–2643.
- [12] Washington K, Berlin J, Branton P, Burgart LJ, Carter DK, Compton CC, Fitzgibbons P, Frankel WL, Jessup J, and Kakar S, et al (2017). Protocol for the Examination of Specimens from Patients with Carcinoma of the Exocrine Pancreas. CAP; [www.cap.org/cancerprotocols; Pancreas Exocrine 3.2.0.1].
- [13] Chen X, Oshima K, Schott D, Wu H, Hall W, Song Y, Tao Y, Li D, Zheng C, and Knechtges P, et al (2017). Assessment of treatment response during chemoradiation therapy for pancreatic cancer based on quantitative radiomic analysis of daily CTs: An exploratory study. *PLoS One*. <https://doi.org/10.1371/journal.pone.0178961>.
- [14] Dalah E, Moraru I, Paulson E, Erickson B, and Li XA (2014). Variability of target and normal structure delineation using multimodality imaging for radiation therapy of pancreatic cancer. *Int J Radiat Oncol Biol Phys*. <https://doi.org/10.1016/j.ijrobp.2014.02.035>.
- [15] Olson P and Hanahan D (2009). Breaching the Cancer Fortress. *Science* **324**, 1400–1401.
- [16] Isa AY, Ward TH, West CML, Slevin NJ, and Homer JJ (2006). Hypoxia In Head And Neck Cancer. *Br J Radiol*. <https://doi.org/10.1259/bjri/17904358>.
- [17] Muraoka N, Uematsu H, Kimura H, Imamura Y, Fujiwara Y, Murakami M, Yamaguchi A, and Itoh H (2008). Apparent Diffusion Coefficient in Pancreatic Cancer: Characterization and Histopathological Correlations. *J Magn Reson Imaging* **27**, 1302–1308.
- [18] Niwa T, Ueno M, Ohkawa S, Yoshida T, Doiuchi T, Ito K, and Inoue T (2009). Advanced Pancreatic Cancer: The Use Of The Apparent Diffusion Coefficient To Predict Response To Chemotherapy. *Br J Radiol* **82**, 28–34.
- [19] Kurosawa J, Tawada K, Mikata R, Ishihara T, Tsuyuguchi T, Saito M, Shimofusa R, Yoshitomi H, Ohtsuka M, and Miyazaki M, et al (2015). Prognostic Relevance of Apparent Diffusion Coefficient Obtained by Diffusion-Weighted MRI in Pancreatic Cancer. *J Magn Reson Imaging* **42**, 1532–1537.
- [20] Nishiofuku H, Tanaka T, Marugami N, Sho M, Akahori T, Nakajima Y, and Kichikawa K (2016). Increase Tumor ADC Value During Chemotherapy Predicts Improved Survival In Unresectable Pancreatic Cancer. *Eur Radiol* **26**(6), 1835–1842. <https://doi.org/10.1007/s00330-015-3999-2>.